Geophysical Research Letters

RESEARCH LETTER
10.1029/2024GL110021

An Observation-Based Estimate of Atlantic Meridional Freshwater Transport

Huayi Zheng[1,2], Lijing Cheng[1,2], Feili Li[3], Yuying Pan[1,2], and Chenyu Zhu[1]

[1]Key Laboratory of Earth System Numerical Modeling and Application, Institute of Atmospheric Physics, Chinese Academy of Sciences, Beijing, China, [2]University of Chinese Academy of Sciences, Beijing, China, [3]State Key Laboratory of Marine Environmental Science & College of Ocean and Earth Sciences, Xiamen University, Xiamen, China

Abstract Meridional freshwater transport (MFT) in the Atlantic Ocean (Atlantic meridional freshwater transport (AMFT)) plays a vital role in the Atlantic Ocean circulations, but an accurate estimate of AMFT time series remains challenging. This study uses an indirect approach that combines ocean salinity, surface evaporation and precipitation observations to derive AMFT and its uncertainty by solving the ocean freshwater budget equation. Climatologically, AMFT is southward between 18.5°S and 34.5°S, but northward from 18.5°S to 66.5°N. AMFT also shows substantial inter-annual variability with a clear separation at ~40°N and is more coincident with the Atlantic Meridional Overturning Circulation (AMOC) at 26°N than 47°N across latitudes. The derived time series indicates that throughout the Atlantic Ocean, there is a positive trend in the AMFT from 2004 to 2020, resulting in an AMFT convergence in the tropical Atlantic and an AMFT divergence in the subtropical North Atlantic.

Plain Language Summary Oceanic freshwater movement plays a crucial role in Earth's climate system. Our study focuses on understanding freshwater flows within the Atlantic Ocean, that is, meridional freshwater transport (AMFT), which is highly relevant to the stability of the Atlantic Meridional Overturning Circulation (AMOC). An indirect and observation-based approach is proposed that allows estimation of the AMFT time series and quantification of the mean state, inter-annual variability, and the trend of the AMFT. The climatological freshwater transport shows that the Atlantic Ocean moves freshwater northward south of 18.5°S, and moves freshwater southward from 18.5°S to 66.5°N. Atlantic meridional freshwater transport in the subtropical North Atlantic is closely related to the AMOC at 26°N, while the link is much weaker in the subpolar North Atlantic. Although the time series is short, it shows a positive trend of the AMFT from 2004 to 2020.

Key Points:

- Observation data are used to estimate Atlantic meridional freshwater transport (AMFT) time series based on the freshwater budget
- On average (climatology), the Atlantic transports freshwater southward north of 18.5°S and northward south of 18.5°S
- From 2004 to 2020, AMFT showed a consistent positive trend across the Atlantic Ocean

Supporting Information:

Supporting Information may be found in the online version of this article.

Correspondence to:

L. Cheng,
chenglij@mail.iap.ac.cn

Citation:

Zheng, H., Cheng, L., Li, F., Pan, Y., & Zhu, C. (2024). An observation-based estimate of Atlantic meridional freshwater transport. *Geophysical Research Letters*, *51*, e2024GL110021. https://doi.org/10.1029/2024GL110021

Received 1 MAY 2024
Accepted 24 NOV 2024

1. Introduction

The Atlantic Ocean circulation is characterized by a northward flow in the upper limb (above about 1,000 m) and a southward flow in the lower limb, known as the Atlantic Meridional Overturning Circulation (AMOC) (Lozier, 2012; Srokosz et al., 2012). This overturning circulation and the salinity distribution largely influence the Atlantic meridional freshwater transport (AMFT) (Haines et al., 2022; Mignac et al., 2019). Here, freshwater transport refers to the freshwater portion of ocean volume transport, as seawater is a mixture of 96.5% freshwater and 3.5% salt. The ocean exchanges freshwater with the atmosphere via evaporation and precipitation at the air-sea interface and also with its adjacent ocean volumes via oceanic processes such as advection, mixing, etc. These exchanges lead to changes in the salinity.

The AMFT is a crucial factor influencing the strength and stability of the AMOC (Hawkins et al., 2011). A weakening of the AMOC leads to a weaker AMFT due to reduced flow. The weaker AMFT will reduce the density difference between the subpolar and subtropical North Atlantic, further intensifying the weakening of AMFT in return. This hypothetical positive feedback associated with AMFT is called the "salt advection feedback" (Stommel, 1961), which is yet to be proven for the real ocean. Additionally, prior studies have indicated that the stability of the AMOC is influenced by the overturning part of the AMFT at the southern boundary of the Atlantic Ocean. If the overturning part of the AMFT is northward, AMOC is monostable; if it is southward, AMOC becomes bistable (de Vries & Weber, 2005; Rahmstorf, 1996; Weijer et al., 2019). This feedback indicates a potentially important role of the AMFT in the stability of the AMOC.

Given the crucial role of AMFT in the AMOC and global climate, it is vital to monitor AMFT and its changes. The most widely used approach relies on direct observations, including data from observing arrays and hydrographic

cruises (Frajka-Williams et al., 2019). Observing arrays, such as the RAPID-MOCHA-WBTS (RAPID—Meridional Overturning Circulation and Heat flux Array—Western Boundary Time Series) array (hereafter referred to as the RAPID array), the Overturning in the Subpolar North Atlantic Program (OSNAP) and the North Atlantic Changes (NOAC) array, consisting of full-depth moorings and gliders deployed across the Atlantic Ocean (F. Li et al., 2021; Lozier et al., 2019; McDonagh et al., 2015; Wett et al., 2023a). These arrays continuously monitor changes in the full-depth ocean temperature, salinity, and velocity to estimate AMFT. The RAPID array observed AMFT at 26.5°N as a mean transport of -0.37 ± 0.20 Sv, with its changes closely correlated with the AMOC (McDonagh et al., 2015). OSNAP observed an average AMFT of -0.33 ± 0.01 Sv (Lozier et al., 2019). Fu et al. (2023) examined the seasonal cycle of AMFT based on OSNAP observations, revealing a maximum strength in winter and a lowest strength in spring and summer.

Hydrographic cruises are conducted as part of large-scale oceanographic programs, such as the World Ocean Circulation Experiment (WOCE) (Ganachaud & Wunsch, 2003) and the Global Ocean Ship-Based Hydrographic Investigations Program (GO-SHIP) (Talley et al., 2016). During these cruises, water properties are sampled at various depths throughout the water column in major ocean basins and regions with distinct water characteristics. Caínzos et al. (2022) analyzed hydrographic data for the past 30 years to estimate AMFT at specific latitudes (30°S, 24°S, 19°S, 11°S, 24°N, 36°N, 47°N, 55°N) in decadal time scale. They observed a weakening trend in the AMFT at 30°S, decreasing from 0.28 ± 0.08 Sv during 1990–1999 to 0.08 ± 0.06 Sv during 2000–2009. However, estimates based on these observing arrays are limited by their spatiotemporal coverage and can only provide observations at specific latitudes. Moreover, the hydrographic cruises do not have velocity measurements, providing an additional source of errors (Wunsch, 1996).

Model or reanalysis data have also been widely used to investigate the variation of the AMFT (Liu et al., 2023; Skliris et al., 2020). Reanalysis data involves the integration of historical observations with numerical models, which results in a consistent and homogeneous global data set of full-depth oceanic variables over a long period (Storto et al., 2019). In Jackson et al. (2019), eight reanalysis data sets were analyzed for the AMFT. While similar climatological AMFT patterns were observed across various products, differences in magnitudes were evident. For instance, all products indicated the strongest southward AMFT around 35–45°N, yet the magnitudes ranged from -0.3 to -0.8 Sv (which will be analyzed in this study in the following section). Compared with observations, reanalysis data revealed a weaker correlation between the AMFT and the AMOC at 26.5°N (Jackson et al., 2019; McDonagh et al., 2015). The limitations of reanalysis data include the spatial and vertical resolution constraints that may prevent it from capturing small-scale processes like eddies, which are crucial for our understanding of the AMOC (Hirschi et al., 2020). Additionally, model drift occurs, especially in poorly sampled regions such as the deep ocean below 2,000 m (Lellouche et al., 2018).

This study provides an estimation of AMFT by solving the ocean freshwater budget in the Atlantic Ocean: we integrate the AMFT given by the RAPID array at ∼26.5°N (McDonagh et al., 2015) southward and northward in combination with ocean freshwater content (calculated by salinity) and surface freshwater flux, with the residual of the freshwater budget equation being the AMFT. The residual approach has been validated in climate models (H. Li et al., 2021). This approach complements existing methods (Frajka-Williams et al., 2019) in various ways. First, it provides AMFT estimates at any latitude, yielding a more complete picture than direct observations (made by observing arrays or hydrological cruises). Therefore, the resultant estimates can support the future understanding of regional patterns and the temporal-spatial propagation of AMFT changes. Second, being model-independent, our AMFT estimates can provide a good basis for climate model evaluation and refinement.

2. Data and Methods

Salinity observations used in this study are from the Institute of Atmospheric Physics (IAP) gridded product (Cheng et al., 2020) with $1° \times 1°$ horizontal resolution and 41 vertical levels for the upper 0–2,000 m. This data set comprises quality-controlled observations from various measurements, including Argo floats, conductivity–temperature–depth (CTD) salinity sensors, bottles, and moorings sourced from the World Ocean Database (WOD) (Boyer et al., 2018). Precipitation and evaporation observations are derived from the Global Precipitation Climatology Project (GPCP) (Adler et al., 2018) and the Objectively Analyzed air-sea Flux (OAflux) (Yu & Weller, 2007), respectively. The GPCP precipitation data has a horizontal resolution of $2.5° \times 2.5°$ since 1980 and is derived from a combination of satellite observations, rain gauge stations, and sounding observations. OAflux evaporation has a resolution of $1° \times 1°$ horizontally since 1958. The evaporation data from OAflux is

parameterized using flux-related variables such as wind speed, sea surface temperature (SST), near-surface air humidity, and temperature, all of which are observed by satellites. To test the robustness of the results, the precipitation and evaporation from the Fifth-generation Reanalysis product of the European Center for Medium Range Weather Forecasts (ERA5) (Hersbach et al., 2020) and the Japanese 55-year Reanalysis (JRA-55) (Kobayashi et al., 2015) reanalysis data is also used (results are presented Figure S1 in Supporting Information S1). ERA5 has a resolution of 0.25° × 0.25° since 1940, whereas JRA-55 has a resolution of 2.5° × 0.25° horizontally since 1958. As surface freshwater flux data sets have higher uncertainty, we have tested all our results using these different data sets. We find that they show consistent estimates of AMFT (Figure S1 in Supporting Information S1), increasing the confidence of our interpretation.

River runoff observations are from Dai (2021), which record the world's largest 921 rivers and provide freshwater exchange data between ocean and land. All data cover the globe with monthly resolution.

Ocean freshwater content (FWC) is calculated from ocean salinity:

$$\mathrm{FWC} = \int_{\varphi_1}^{\varphi} \int_{x_e}^{x_w} \int_{\mathrm{depth}}^{0} -\frac{S}{S_{\mathrm{ref}}} dz dx dy \tag{1}$$

where depth is ocean depth, x_w and x_e denote the west and east boundary of the Atlantic Ocean, respectively. The FWC is calculated based on the upper 2,000 m salinity, aligning with the Argo network's maximum observation depth. Additionally, the magnitude of salinity changes decreases rapidly with depth in the ocean, making the upper 2,000 m FWC changes well representative of the full-depth FWC changes. This choice does not impact the conclusion after a test using full-depth reanalysis data sets. S_{ref} is a reference salinity chosen as 35 g/kg. Previous studies have discussed the limitation of using an arbitrary choice of S_{ref} on AMFT estimation (Schauer & Losch, 2019). However, the choice of reference salinity is found to have a negligible impact on the AMFT estimates in this study (Figure S2 in Supporting Information S1). Using more theoretically correct definition of ($\mathrm{FWC} = 1 - 10^{-3}S$) will need to be explored in the future.

The Atlantic Ocean freshwater budget is described by:

$$\frac{\mathrm{dFWC}}{dt} = \int_{\varphi_1}^{\varphi} \int_{x_e}^{x_w} (P + R - E)\, dx dy + \mathrm{AMFT}_{\varphi_1} - \mathrm{AMFT}(\varphi) \tag{2}$$

where P is precipitation, E is evaporation, R is river runoff and $\mathrm{AMFT}_{\varphi_1} - \mathrm{AMFT}(\varphi)$ is the convergence of the AMFT. To derive AMFT, Equation 2 can be rewritten as

$$\mathrm{AMFT}(\varphi) = \int_{\varphi_1}^{\varphi} \int_{x_e}^{x_w} (P + R - E)\, dx dy - \frac{\mathrm{dFWC}}{dt} + \mathrm{AMFT}_{\varphi_1} \tag{3}$$

where φ_1 is the start of integration latitude, and there is a direct observational array (The RAPID array observations at 26.5°N are used in this study) and φ is the target latitude. To reduce high-frequency (month-to-month) noise in the calculation of the time derivative of the FWC (dFWC/dt), a 13-point weighted running smoothing is applied (the weights are [1/576,6/576,19/576,42/576,71/576,96/576,106/576,96/576,71/576,42/576,19/576,6/576,1/576]) (Cheng et al., 2019; Trenberth et al., 2007). The weak freshwater exchange (0.03 Sv) (Criado-Aldeanueva et al., 2012) between the Atlantic and the Mediterranean via the Strait of Gibraltar is ignored. For inter-annual variability, we calculate anomalies from original time series by subtracting the 12 monthly climatologies relative to 2004–2020. The anomalies are smoothed by calculating 5-month running means, with different weights for different months: [1/12,3/12,4/12,3/12,1/12]. Integrating the right-hand side in Equation 3 from 26.5°N southward and northward allows the derivation of the AMFT at any latitude. In previous estimates of the mean state of the AMFT (Wijffels, 2001; Wijffels et al., 1992), the Bering Strait was selected as the starting integration location, primarily due to the availability of observed AMFT data there (Woodgate, 2018).

In this study, the latitude φ_1 is set as 26.5°N because: (a) The RAPID array provides a valuable direct observation of AMFT at 26.5°N (McDonagh et al., 2015) and (b) this choice avoids integrating the polar areas where salinity observations are sparse. By integrating Equation 3 from 26.5°N, the study takes advantage of more reliable

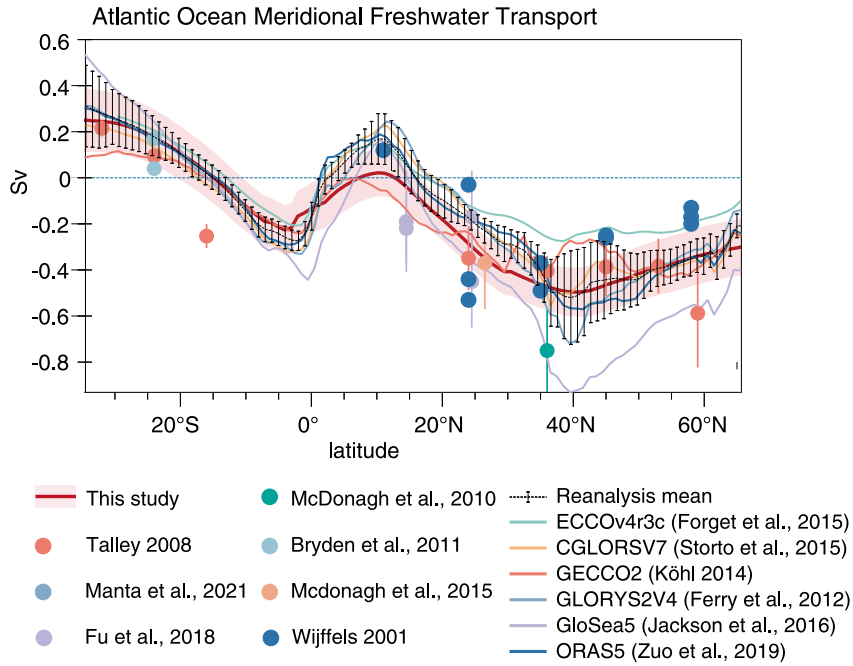

Figure 1. The Climatology of Atlantic meridional freshwater transport from this study (red thick line), from direct observation (dot) (Bryden et al., 2010, 2011; Fu et al., 2018; Manta et al., 2021; McDonagh et al., 2015; Talley, 2008; Wijffels, 2001), and reanalysis data (thin lines) (Ferry et al., 2012; Forget et al., 2015; Jackson et al., 2016; Köhl, 2014; Storto et al., 2015; Zuo et al., 2019). Shading is the uncertainty of this study based on the Monte Carlo approach (Figures S4 and S5 in Supporting Information S1). The positive values mean northward transport and the negative values mean southward transport.

observations in the low and middle latitudes. Specifically, we focus on the Atlantic regions between 34.5°S and 66.5°N. The AMFT at 26.5°N published by the RAPID array is limited to 2004–2012. To provide a longer time series of the AMFT, reconstructed AMFT at 26.5°N from 2004 to 2020 is developed based on the linear regression between AMFT and the AMOC. The reconstruction of AMFT at 26.5°N is strongly correlated (correlation coefficient = 0.97) with direct observation (Figure S3 in Supporting Information S1).

The uncertainty of the AMFT is quantified using a Monte Carlo approach to propagate all sources of errors into the final estimates (Figures S4 and S5 in Supporting Information S1). Specifically, for precipitation, evaporation and $AMFT_{26.5°N}$, we adopt the error estimates given by GPCP, OAflux, and the RAPID array data sets, respectively. Using these errors and assuming a normal distribution, each month, 100 members are generated for each variable. To account for the uncertainty induced by salinity data, we adopted the ensemble members of the IAP salinity products, which account for the major source of errors in the salinity data set including instrumental and sampling/gap-filling errors (Cheng et al., 2020; Cheng & Zhu, 2016). River runoff uncertainty is neglected due to its minor contribution. With these ensembles from each variable, the uncertainty of AMFT is calculated as follows. Each time, we select one member from GPCP, OAflux, the RAPID array, and salinity data and then derive the AMFT estimate. This process is repeated 100 times, yielding 100 AMFT ensemble members. The standard deviation of these estimates is used as the measure of uncertainty for the AMFT estimation (standard deviation represents a 66% confidence interval). We also tested the influence of ensemble member number on uncertainty robustness and found the maximum difference between uncertainty inferred from 100 members and 300 members is less than 2%. This method assumes independent errors between variables, as they are observed and processed by different systems and groups. With this Monte Carlo approach, we consider all major sources of uncertainty.

3. Climatological Distribution of AMFT

The estimated mean AMFT for 2004–2020 is northward between 34.5°S and 18.5°S and southward between 18.5°S and 66.5°N (Figure 1). The northward AMFT decreases to zero at ~18.5°S, then reverses to a southward transport, reaching a peak of -0.26 ± 0.11 Sv (mean $\pm$ 1σ) around 3.5°S and -0.49 ± 0.11 Sv at 39.5°N.

Our estimation is always within the spread of direct observations (Figure 1). For instance, the AMFT estimate at ~24°N is −0.30 ± 0.10 Sv in this study, −0.03 Sv in (Wijffels (2001)) and −0.53 Sv in (Wijffels (2001)) Sv (Table S1 in Supporting Information S1). The direction of the AMFT is influenced by the vertical structure of ocean circulation and salinity (Mignac et al., 2019). Ocean meridional velocity is northward in the upper 1000 m and returns southward below this depth. The volumes of northward and southward transport are roughly equal, yielding near net-zero volume transport. However, while the volumes of northward and southward transport are roughly equal, the salinity differs between the two flows. Consequently, the FWC of the northward and southward flows is different, resulting in a net AMFT. For example, at 24°N, the upper 1,000 m (northward flow) is saltier than the southward return flow, resulting in less freshwater being transported northward than southward, leading to a net southward AMFT. At 36°N, the salinity difference between the northward and southward parts is stronger than any latitudes from 15° to 65°N because of the intrusion of Mediterranean water (Blanke et al., 2006), so AMFT at 36°N is stronger than other latitudes.

Other observational estimates and reanalysis data from Jackson et al. (2019) are also shown together with our estimate in Figure 1. The reanalysis data exhibit a similar pattern of AMFT compared to our estimate; however, some significant differences occur. For instance, the reanalysis-based AMFT is higher than our estimates from 0° to 35°N. This could be associated with salinity biases in reanalysis data seen in previous studies (Mignac et al., 2019). Notably, a larger spread occurs between 35°N and 60°N for reanalysis data than other latitudes. GECCO2 is the closest to our estimate.

4. Inter-Annual Variability of AMFT

To examine the inter-annual variation of the AMFT, a Hovmöller diagram of AMFT anomalies is provided in Figure 2a. The variability of AMFT across the Atlantic Ocean reveals potential links between the AMFT at different latitudes and a clear separation of changes around 40°N. Specifically, south of 40°N, the variability of AMFT shows consistent changes across various latitudes. Similarly, north of 40°N, the AMFT displays strong coherence. The cross-correlations are performed to better illustrate the coherence (Figure 2b). Since the focus here is on inter-annual variability, we use detrended AMFT. The cross-correlations between any two latitudes show that the largest spread of strong coherence (correlation >0.9) occurs at 20.5°S, spanning from 34.5°S to 3.5°N, while the smallest spread occurs at 33.5°N, spanning from 28.5°N to 37.5°N. The AMFT north of 40°N is predominantly influenced by gyre circulation, whereas south of 40°N, the AMOC plays a more crucial role (Liu et al., 2023). These regional impacts result in discontinuity near 40°N of the AMFT potentially.

A similar pattern of discontinuity near 40°N, or between the subtropical and subpolar North Atlantic, is also found in the AMOC (Bingham et al., 2007; Jackson et al., 2022) and the Atlantic meridional heat transport (Kelly et al., 2014). Several factors were proposed to explain this discontinuity: (a) The slow southward propagation from the subpolar to subtropical North Atlantic, which can take several years (J. Zhang & Zhang, 2015; R. Zhang, 2010); (b) different drivers for subpolar and subtropical AMOC changes (Asbjørnsen et al., 2024; Jackson et al., 2022); and (c) the discrepancy in measuring methodology can contribute to observation errors (Frajka-Williams et al., 2023). However, the exact drivers remain unclear.

The latitude-dependent relationship between detrended AMFT and the AMOC is illustrated in Figure 2c, with observed MOC values at 26.5°N (Moat et al., 2020) and 47°N (Wett et al., 2023a). The AMFT across the Atlantic Ocean is negatively correlated with 26.5°N MOC and passes a significance test at the 99% level. The maximum correlation occurs at 26.5°N, and reduces poleward. The correlation reaches −0.35 at 34.5°S and −0.31 at 65.5°N. It is interesting to note that the AMFT in the South Atlantic is significantly correlated with the AMOC at 26.5°N with ~0.4 within 10°–20°S. This suggests that AMOC in the North Atlantic might have a remote influence on the AMFT in the South Atlantic, consistent with findings from previous studies by Zhu et al. (2020, 2023). It has been noted that changes in AMOC in the North Atlantic, including at 26.5°N, can propagate to the South Atlantic and subsequently influence local AMFT through Rossby waves and Kelvin waves, as suggested by Johnson and Marshall (2002). The mechanism, however, requires further exploration. The complexity is that not only the AMOC, but also the gyre circulation can impact the AMFT in the low-latitudes. Interestingly, the correlations between MOC at 47°N and AMFT at different latitudes are weak, with a maximum correlation of −0.35 at ~5°N. It remains an open question why the MOC at 47°N has significant correlations with AMFT within 20°S–20°N. Previous studies have found MOC at 26.5°N is synchronously coherent (lag = 0) from 0° to 40°N, while the MOC at 47°N aligns with the MOC between 47°N and 66.5°N (Bingham et al., 2007). This suggests that the AMOC at

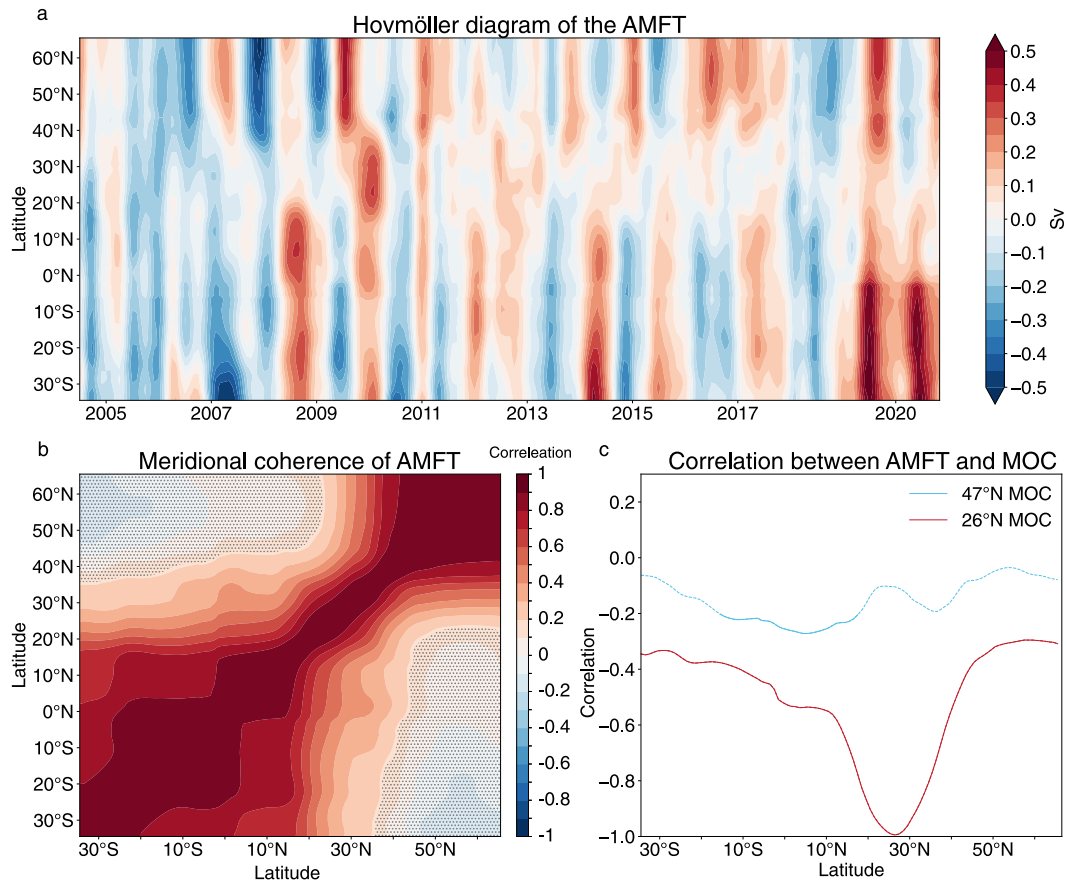

Figure 2. (a) Hovmöller diagram of the zonal sum Atlantic meridional freshwater transport (AMFT) anomalies relative to 2004–2020 monthly climatology. (b) Cross correlation of the detrended AMFT between different latitudes based on 2004–2020. The stipples indicate signals that are insignificant (at 99% confidence level). (c) The correlation between AMFT across the Atlantic Ocean and 26.5°N (blue line) and 47°N MOC (orange line). The solid lines are showed for the correlation pass 99% confidence test, while dashed lines indicate trends that do not pass significance test at 99% confidence level. AMFT and Atlantic Meridional Overturning Circulation are detrended to avoid the influence of trends.

26.5°N represents conditions in the subtropical region, whereas the AMOC at 47°N reflects those in the subpolar North Atlantic. The AMFT is controlled by gyres instead of the AMOC in the subpolar North Atlantic (40°N–66.5°N) (Liu et al., 2023), so AMFT is decorrelated with MOC at 26.5°N and 47°N. In the subtropics, AMFT is dominated by the AMOC, resulting in a negative correlation due to the salty northward limb and fresh southward limb. The relationship between the AMFT and its driving mechanisms in the South Atlantic remains uncertain.

5. Trend of the AMFT

The trend of the AMFT from 2004 to 2020 is also evaluated despite the short time series (Figure 3). It shows a consistent positive trend of the AMFT across the Atlantic Ocean, which means either a decrease of southward AMFT or an increase of northward AMFT depending on the climatology of AMFT (Figure 1). For instance, the trends of AMFT at 30.5°S,15.5°S, 20.5°N and 40.5°N are 0.18 ± 0.05, 0.18 ± 0.05, 0.05 ± 0.03, and 0.08 ± 0.04 Sv decade^{-1} respectively (90% confidence interval according to the Student's *t*-test).

Here, we separate the Atlantic Ocean into several parts, the South Atlantic (15.5°–30.5°S), tropical Atlantic (15.5°S–20.5°N) and subtropical North Atlantic (20.5°–40.5°N) to explore the contribution of AMFT convergence and surface freshwater flux to FWC acceleration (the derivative of the FWC time derivative). Positive acceleration indicates either a slowing of the downward trend or an increase upward trend in FWC, whereas negative acceleration, or deceleration, implies the opposite. Uncertainty in the FWC acceleration is evaluated using a 90% confidence interval according to the Student's *t*-test. In the South Atlantic, there is a negative FWC acceleration of

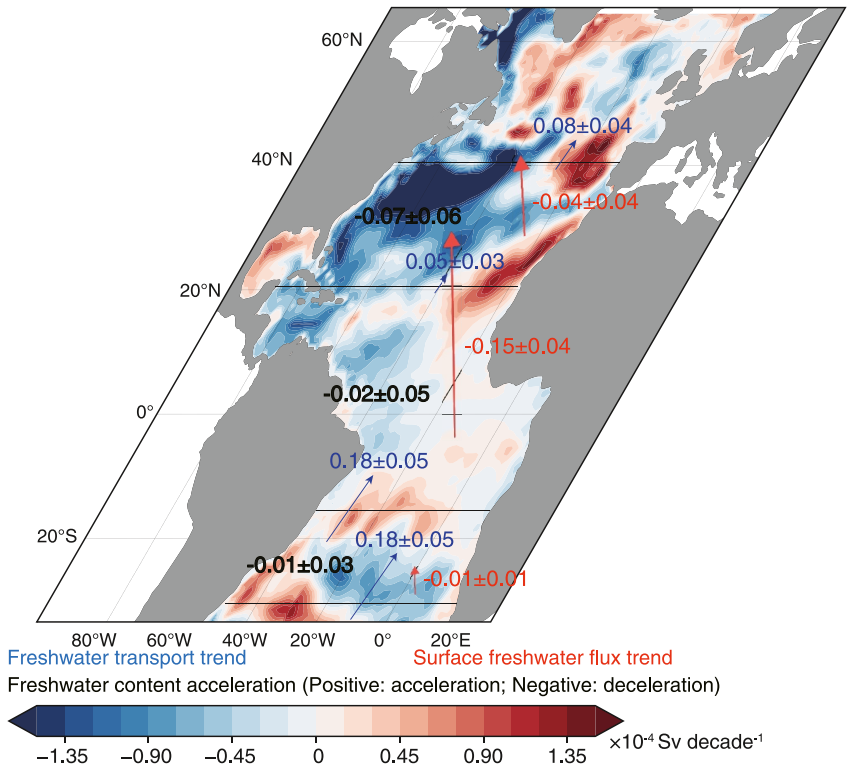

Figure 3. The acceleration of ocean freshwater content in each 1° grid is shown in color shading (the black numbers are the trend in each box isolated by the black line); the Atlantic meridional freshwater transport (AMFT) trends shown in blue arrows and blue numbers in each box (with positive northward), and the surface freshwater flux trends shown in red arrows and red numbers (with positive downward into the ocean). The unit of the number is Sv decade^{-1}. All trends are calculated from 2004 to 2020. The size of the arrows also indicates the magnitude of the AMFT trend. The South Atlantic, tropical and subtropical North Atlantic are divided by black lines.

-0.01 ± 0.03 Sv decade^{-1}, primarily driven by surface freshwater flux (-0.01 ± 0.01 Sv decade^{-1}), with a negligible contribution from AMFT convergence (0.00 ± 0.02 Sv decade^{-1}). In the tropical Atlantic, FWC changes show an acceleration of -0.02 ± 0.05 Sv decade^{-1}, mainly due to a decreasing surface freshwater input (-0.15 ± 0.04 Sv decade^{-1}), with an increasing contribution from AMFT convergence (0.13 ± 0.04 Sv decade^{-1}). FWC in the subtropical North Atlantic decelerates (-0.07 ± 0.06 Sv decade^{-1}), largely driven by AMFT convergence (-0.03 ± 0.04 Sv decade^{-1}) and surface freshwater flux (-0.04 ± 0.04 Sv decade^{-1}).

Our results above are in line with previous model or reanalysis-based estimates. For instance, Kelly et al. (2016) simulated AMFT trends during 2004–2012 using a model and found a positive trend across the Atlantic Ocean. The northward AMFT observed by the RAPID array at 26.5°N increased at a rate of 0.23 Sv decade^{-1} from 2004 to 2012, consistent with our study (McDonagh et al., 2015). A tracer-percentile analytic framework also suggests a global-scale enhanced poleward freshwater transport because of the global water cycle amplification (Sohail et al., 2022).

6. Conclusions and Discussion

A residual approach is used to estimate the AMFT from 2004 to 2020. The method is based on a budget conservation equation and takes advantage of recent high-quality observations and physical constraints to estimate AMFT, which complements estimates from direct observations only available at selected latitudes or from reanalysis products. This approach allows an estimate of the AMFT time series, contributing to the investigation of the climatology, inter-annual variability, and trend. The results contribute to the understanding of the ocean component of the global freshwater cycle and have implications for model evaluation and development.

Climatologically, the Atlantic Ocean shows a strong southward AMFT between 18.5°S and 66.5°N, and a northward AMFT from 18.5°S to 34.5°S. The transport maximum occurs at 3.5°S (-0.26 ± 0.09 Sv) and 39.5°N

(−0.49 ± 0.08 Sv). Reanalysis data show higher AMFT from 0° to 35°N than our estimates (Figure 1). Previous studies have shown that reanalysis data tend to underestimate the southward overturning part of AMFT associated with salinity bias, resulting in higher values of AMFT (Mignac et al., 2019). The large spread of AMFT from various reanalyzes data between 35°N and 50°N raises concerns about the accuracy of these reanalyzes. This uncertainty might be linked to the complex ocean topography, river runoff or sparse observations. The model resolution might also be an important factor, as only high-resolution reanalyzes can resolve mesoscale features.

The new estimates in this study complement the current direct observations based on arrays and hydrological sections. Because the array observations are only available through several sections like the RAPID array and OSNAP, hydrographic sections often provide time-discrete observations; by providing AMFT time series at any latitude, the estimates of this study provide a more complete temporal and spatial data set, making it suitable for exploring the spatial-temporal variations of the AMFT.

The inter-annual variability based on the residual method is also shown in this study (Figure 2a). AMFT exhibits significant inter-annual variability, with noticeable distinctions between the northern and southern regions separated roughly at ∼40°N (Figure 2b). The distinctions may be explained by the relative contribution of gyre and overturning to AMFT. Correlation analysis highlights a weak link between 47°N MOC and AMFT in the region north of 40°N, indicating gyre AMFT dominance, whereas a strong link between the AMFT in subtropical North Atlantic and 26.5°N MOC suggests the key role of overturning AMFT (Figure 2c).

From 2004 to 2020, AMFT showed a consistent positive trend across the Atlantic Ocean (Figure 3). These findings align with previous studies, such as Kelly et al. (2016) and McDonagh et al. (2015), which also observed increased northward AMFT. The driver of AMFT's positive trend is still unclear and needs further exploration. Analysis of the South, tropical, and subtropical North Atlantic reveals that both AMFT convergence and surface freshwater fluxes contribute to FWC acceleration. All three regions exhibited a deceleration in FWC changes, though the changes in the South and tropical Atlantic are small and insignificant. The deceleration of the FWC change is consistent with the observed slowdown in salinity pattern amplification (Vinogradova & Ponte, 2017).

Although this study shows that the AMFT can be inferred using the residual method, the limitation and the uncertainty in the inferred AMFT still exist. The analysis excludes freshwater from sea ice, which is crucial for the Atlantic freshwater budget in high latitudes, and its impact will be evaluated in future research. The uncertainty of our estimate arises from multiple sources: salinity products, surface freshwater flux, and the AMFT at 26.5°N. We indicated Figure S1 in Supporting Information S1 that using different surface freshwater flux products do not change the key results of this study, so the primary uncertainty is from salinity products and 26.5°N AMFT estimates. Reducing this uncertainty requires efforts from various perspectives, such as increasing the salinity observations in the future (especially in the eddy-rich regions where there are substantial temporospatial variability), increasing the resolution of the RAPID array etc. Next, it will be very useful to put together various estimates to assess the capability of our understanding of freshwater transport/budget. For instance, integrating the FWC from the RAPID array AMFT to the OSNAP latitude and comparing the derived AMFT with the OSNAP-based estimates. A similar comparison can also be made with the derived AMFT from the hydrological section, models and reanalysis. Putting these estimates together could cross-evaluate different approaches and strengthen evidence of our understanding of an oceanic part of the water cycle.

Data Availability Statement

AMFT produced in this study is available at https://doi.org/10.5281/zenodo.12790901 (Zheng, 2024). IAP salinity data are available from http://www.ocean.iap.ac.cn/ftp/cheng/CZ16_v0_IAP_Salinity_gridded_1month_netcdf/ (Cheng et al., 2020). The GPCP precipitation data and OAflux evaporation data were collected from https://www.ncei.noaa.gov/products/global-precipitation-climatology-project (Adler et al., 2018) and https://oaflux.whoi.edu/data-access/ (Yu & Weller, 2007), respectively. The ERA5 data and JRA-55 data are available from https://doi.org/10.24381/cds.f17050d7 (Hersbach et al., 2023) and https://climatedataguide.ucar.edu/climate-data/jra-55 (Kobayashi et al., 2015). The river runoff data is freely available at https://www.atmos.albany.edu/facstaff/adai/ (Dai, 2021). The RAPID AMFT data is available from McDonagh et al. (2015). The reanalysis data for comparison in Figure 1 were downloaded from https://doi.org/10.5281/zenodo.2598509 (Jackson, 2019). The MOC at 26.5°N and 47°N are sourced from https://rapid.ac.uk/ (Moat et al., 2020) and https://doi.pangaea.de/10.1594/PANGAEA.959558 (Wett et al., 2023b).

Acknowledgments
This study was supported by the National Natural Science Foundation of China (Grant 42122046, 42076202, 42075036), National Key Scientific and Technological Infrastructure project "Earth System Science Numerical Simulator Facility" (EarthLab) and the new Cornerstone Science Foundation through the XPLORER PRIZE. F. Li acknowledges the financial support from the National Key R&D Program of China (Grant 2023YFF0805102). Gratitude is extended to Elaine L. McDonagh, who graciously shared RAPID freshwater transport data. We also thank two anonymous reviewers for their detailed and constructive comments.

References

Adler, R. F., Sapiano, M., Huffman, G. J., Wang, J., Gu, G., Bolvin, D., et al. (2018). The Global Precipitation Climatology Project (GPCP) monthly analysis (new version 2.3) and a review of 2017 global precipitation. *Atmosphere*, *9*(4), 138. https://doi.org/10.3390/atmos9040138

Asbjørnsen, H., Eldevik, T., Skrefsrud, J., Johnson, H. L., & Sanchez-Franks, A. (2024). Observed change and the extent of coherence in the Gulf Stream system. *Ocean Science*, *20*(3), 799–816. https://doi.org/10.5194/os-20-799-2024

Bingham, R. J., Hughes, C. W., Roussenov, V., & Williams, R. G. (2007). Meridional coherence of the North Atlantic meridional overturning circulation. *Geophysical Research Letters*, *34*(23). https://doi.org/10.1029/2007gl031731

Blanke, B., Arhan, M., & Speich, S. (2006). Salinity changes along the upper limb of the Atlantic thermohaline circulation. *Geophysical Research Letters*, *33*(6). https://doi.org/10.1029/2005gl024938

Boyer, T. P., Baranova, O. K., Coleman, C., Garcia, H. E., Grodsky, A., Locarnini, R. A., et al. (2018). NOAA atlas nesdis 87. *World Ocean Database*, 1–207.

Bryden, H. L., King, B. A., & McCarthy, G. D. (2011). South Atlantic overturning circulation at 24°S. *Journal of Marine Research*, *69*(1), 38–55. https://doi.org/10.1357/002224011798147633

Bryden, H. L., King, B. A., McLeod, P., McDonagh, E. L., & Valdés, S. T. (2010). Circulation, heat, and freshwater transport at 36°N in the Atlantic. *Journal of Physical Oceanography*, *40*(12), 2661–2678. https://doi.org/10.1175/2010jpo4176.1

Caínzos, V., Hernández-Guerra, A., McCarthy, G. D., McDonagh, E. L., Cubas Armas, M., & Pérez-Hernández, M. D. (2022). Thirty years of GOSHIP and WOCE data: Atlantic overturning of mass, heat, and freshwater transport. *Geophysical Research Letters*, *49*(4). https://doi.org/10.1029/2021gl096527

Cheng, L., Trenberth, K. E., Fasullo, J. T., Mayer, M., Balmaseda, M., & Zhu, J. (2019). Evolution of ocean heat content related to ENSO. *Journal of Climate*, *32*(12), 3529–3556. https://doi.org/10.1175/jcli-d-18-0607.1

Cheng, L., Trenberth, K. E., Gruber, N., Abraham, J. P., Fasullo, J. T., Li, G., et al. (2020). Improved estimates of changes in upper ocean salinity and the hydrological cycle. *Journal of Climate*, *33*(23), 10357–10381. https://doi.org/10.1175/jcli-d-20-0366.1

Cheng, L., & Zhu, J. (2016). Benefits of CMIP5 multimodel ensemble in reconstructing historical ocean subsurface temperature variations. *Journal of Climate*, *29*(15), 5393–5416. https://doi.org/10.1175/jcli-d-15-0730.1

Criado-Aldeanueva, F., Soto-Navarro, F. J., & García-Lafuente, J. (2012). Seasonal and interannual variability of surface heat and freshwater fluxes in the Mediterranean Sea: Budgets and exchange through the Strait of Gibraltar. *International Journal of Climatology*, *32*(2), 286–302. https://doi.org/10.1002/joc.2268

Dai, A. G. (2021). Hydroclimatic trends during 1950-2018 over global land. *Climate Dynamics*, *56*(11–12), 4027–4049. https://doi.org/10.1007/s00382-021-05684-1

de Vries, P., & Weber, S. L. (2005). The Atlantic freshwater budget as a diagnostic for the existence of a stable shut down of the meridional overturning circulation. *Geophysical Research Letters*, *32*(9). https://doi.org/10.1029/2004gl021450

Ferry, N., Parent, L., Garric, G., Bricaud, C., Testut, C., Le Galloudec, O., et al. (2012). GLORYS2V1 global ocean reanalysis of the altimetric era (1992–2009) at MESO scale. *Mercator Ocean–Quaterly Newsletter*, *44*.

Forget, G., Campin, J. M., Heimbach, P., Hill, C. N., Ponte, R. M., & Wunsch, C. (2015). ECCO version 4: An integrated framework for non-linear inverse modeling and Global Ocean state estimation. *Geoscientific Model Development*, *8*(10), 3071–3104. https://doi.org/10.5194/gmd-8-3071-2015

Frajka-Williams, E., Ansorge, I. J., Baehr, J., Bryden, H. L., Chidichimo, M. P., Cunningham, S. A., et al. (2019). Atlantic meridional overturning circulation: Observed transport and variability. *Frontiers in Marine Science*, *6*. https://doi.org/10.3389/fmars.2019.00260

Frajka-Williams, E., Foukal, N., & Danabasoglu, G. (2023). Should AMOC observations continue: How and why? *Philosophical Transactions of the Royal Society A: Mathematical, Physical & Engineering Sciences*, *381*(2262), 20220195. https://royalsocietypublishing.org/doi/abs/10.1098/rsta.2022.0195

Fu, Y., Karstensen, J., & Brandt, P. (2018). Atlantic meridional overturning circulation at 14.5°N in 1989 and 2013 and 24.5°N in 1992 and 2015: Volume, heat, and freshwater transports. *Ocean Science*, *14*(4), 589–616. https://doi.org/10.5194/os-14-589-2018

Fu, Y., Lozier, M. S., Bilo, T. C., Bower, A. S., Cunningham, S. A., Cyr, F., et al. (2023). Seasonality of the meridional overturning circulation in the subpolar North Atlantic. *Commun Earth Environ*, *4*(1), 181. https://doi.org/10.1038/s43247-023-00848-9

Ganachaud, A., & Wunsch, C. (2003). Large-scale ocean heat and freshwater transports during the world Ocean Circulation experiment. *Journal of Climate*, *16*(4), 696–705. https://doi.org/10.1175/1520-0442(2003)016<0696:lsohaf>2.0.co;2

Haines, K., Ferreira, D., & Mignac, D. (2022). Variability and feedbacks in the Atlantic freshwater budget of CMIP5 models with reference to Atlantic meridional overturning circulation stability. *Frontiers in Marine Science*, *9*. https://doi.org/10.3389/fmars.2022.830821

Hawkins, E., Smith, R. S., Allison, L. C., Gregory, J. M., Woollings, T. J., Pohlmann, H., & de Cuevas, B. (2011). Bistability of the Atlantic overturning circulation in a global climate model and links to ocean freshwater transport. *Geophysical Research Letters*, *38*(10). https://doi.org/10.1029/2011gl047208

Hersbach, H., Bell, B., Berrisford, P., Biavati, G., Horányi, A., Muñoz Sabater, J., et al. (2023). ERA5 monthly averaged data on single levels from 1940 to present [Dataset]. *Copernicus Climate Change Service (C3S) Climate Data Store (CDS)*. https://doi.org/10.24381/cds.f17050d7

Hersbach, H., Bell, B., Berrisford, P., Hirahara, S., Horányi, A., Muñoz-Sabater, J., et al. (2020). The ERA5 global reanalysis. *Quarterly Journal of the Royal Meteorological Society*, *146*(730), 1999–2049. https://doi.org/10.1002/qj.3803

Hirschi, J. J. M., Barnier, B., Böning, C., Biastoch, A., Blaker, A. T., Coward, A., et al. (2020). The Atlantic meridional overturning circulation in high-resolution models. *Journal of Geophysical Research: Oceans*, *125*(4). https://doi.org/10.1029/2019jc015522

Jackson, L. C. (2019). North Atlantic circulation: A perspective from ocean reanalyses (version submission1) [Dataset]. *Zenodo*. https://doi.org/10.5281/zenodo.2598509

Jackson, L. C., Biastoch, A., Buckley, M. W., Desbruyères, D. G., Frajka-Williams, E., Moat, B., & Robson, J. (2022). The evolution of the North Atlantic meridional overturning circulation since 1980. *Nature Reviews Earth and Environment*, *3*(4), 241–254. https://doi.org/10.1038/s43017-022-00263-2

Jackson, L. C., Dubois, C., Forget, G., Haines, K., Harrison, M., Iovino, D., et al. (2019). The mean state and variability of the North Atlantic circulation: A perspective from ocean reanalyses. *Journal of Geophysical Research: Oceans*, *124*(12), 9141–9170. https://doi.org/10.1029/2019jc015210

Jackson, L. C., Peterson, K. A., Roberts, C. D., & Wood, R. A. (2016). Recent slowing of Atlantic overturning circulation as a recovery from earlier strengthening. *Nature Geoscience*, *9*(7), 518–522. https://doi.org/10.1038/ngeo2715

Johnson, H. L., & Marshall, D. P. (2002). A theory for the surface Atlantic response to thermohaline variability. *Journal of Physical Oceanography*, *32*(4), 1121–1132. https://doi.org/10.1175/1520-0485(2002)032<1121:atftsa>2.0.co;2

Kelly, K. A., Drushka, K., Thompson, L., Le Bars, D., & McDonagh, E. L. (2016). Impact of slowdown of Atlantic overturning circulation on heat and freshwater transports. *Geophysical Research Letters*, *43*(14), 7625–7631. https://doi.org/10.1002/2016gl069789

Kelly, K. A., Thompson, L., & Lyman, J. (2014). The coherence and impact of meridional heat transport anomalies in the Atlantic Ocean inferred from observations. *Journal of Climate*, *27*(4), 1469–1487. https://doi.org/10.1175/jcli-d-12-00131.1

Kobayashi, S., Ota, Y., Harada, Y., Ebita, A., Moriya, M., Onoda, H., et al. (2015). The JRA-55 reanalysis: General specifications and basic characteristics. *Journal of the Meteorological Society of Japan. Ser. II*, *93*(1), 5–48. https://doi.org/10.2151/jmsj.2015-001

Köhl, A. (2014). Evaluation of the GECCO2 ocean synthesis: Transports of volume, heat and freshwater in the Atlantic. *Quarterly Journal of the Royal Meteorological Society*, *141*(686), 166–181. https://doi.org/10.1002/qj.2347

Lellouche, J.-M., Greiner, E., Le Galloudec, O., Garric, G., Regnier, C., Drevillon, M., et al. (2018). Recent updates to the Copernicus Marine Service global ocean monitoring and forecasting real-time 1/12° high-resolution system. *Ocean Science*, *14*(5), 1093–1126. https://doi.org/10.5194/os-14-1093-2018

Li, F., Lozier, M. S., Holliday, N. P., Johns, W. E., Le Bras, I. A., Moat, B. I., et al. (2021a). Observation-based estimates of heat and freshwater exchanges from the subtropical North Atlantic to the Arctic. *Progress in Oceanography*, *197*, 102640. https://doi.org/10.1016/j.pocean.2021.102640

Li, H., Fedorov, A., & Liu, W. (2021b). AMOC stability and diverging response to Arctic sea ice decline in two climate models. *Journal of Climate*, *34*(13), 5443–5460.

Liu, X., Köhl, A., & Stammer, D. (2023). Causes for Atlantic freshwater content variability in the GECCO3 ocean synthesis. *Journal of Geophysical Research: Oceans*, *128*(1), e2022JC018796. https://doi.org/10.1029/2022jc018796

Lozier, M. S. (2012). Overturning in the North Atlantic. *Annual Review of Marine Science*, *4*(1), 291–315. https://doi.org/10.1146/annurev-marine-120710-100740

Lozier, M. S., Li, F., Bacon, S., Bahr, F., Bower, A. S., Cunningham, S. A., et al. (2019). A sea change in our view of overturning in the subpolar North Atlantic. *Science*, *363*(6426), 516–521. https://doi.org/10.1126/science.aau6592

Manta, G., Speich, S., Karstensen, J., Hummels, R., Kersalé, M., Laxenaire, R., et al. (2021). The South Atlantic meridional overturning circulation and mesoscale eddies in the first GO-SHIP section at 34.5°S. *Journal of Geophysical Research: Oceans*, *126*(2). https://doi.org/10.1029/2020jc016962

McDonagh, E. L., King, B. A., Bryden, H. L., Courtois, P., Szuts, Z., Baringer, M., et al. (2015). Continuous estimate of Atlantic oceanic freshwater flux at 26.5 N. *Journal of Climate*, *28*(22), 8888–8906. https://doi.org/10.1175/jcli-d-14-00519.1

Mignac, D., Ferreira, D., & Haines, K. (2019). Decoupled freshwater transport and meridional overturning in the South Atlantic. *Geophysical Research Letters*, *46*(4), 2178–2186. https://doi.org/10.1029/2018gl081328

Moat, B. I., Smeed, D. A., Frajka-Williams, E., Desbruyères, D. G., Beaulieu, C., Johns, W. E., et al. (2020). Pending recovery in the strength of the meridional overturning circulation at 26N. *Ocean Science*, *16*(4), 863–874. https://doi.org/10.5194/os-16-863-2020

Rahmstorf, S. (1996). On the freshwater forcing and transport of the Atlantic thermohaline circulation. *Climate Dynamics*, *12*(12), 799–811. https://doi.org/10.1007/s003820050144

Schauer, U., & Losch, M. (2019). "Freshwater" in the ocean is not a useful parameter in climate research. *Journal of Physical Oceanography*, *49*(9), 2309–2321. https://doi.org/10.1175/jpo-d-19-0102.1

Skliris, N., Marsh, R., Mecking, J. V., & Zika, J. D. (2020). Changing water cycle and freshwater transports in the Atlantic Ocean in observations and CMIP5 models. *Climate Dynamics*, *54*(11–12), 4971–4989. https://doi.org/10.1007/s00382-020-05261-y

Sohail, T., Zika, J. D., Irving, D. B., & Church, J. A. (2022). Observed poleward freshwater transport since 1970. *Nature*, *602*(7898), 617–622. https://doi.org/10.1038/s41586-021-04370-w

Srokosz, M., Baringer, M., Bryden, H., Cunningham, S., Delworth, T., Lozier, S., et al. (2012). Past, present, and future changes in the Atlantic meridional overturning circulation. *Bulletin of the American Meteorological Society*, *93*(11), 1663–1676. https://doi.org/10.1175/bams-d-11-00151.1

Stommel, H. (1961). Thermohaline convection with two stable regimes of flow. *Tellus*, *13*(2), 224–230. https://doi.org/10.3402/tellusb.v13i2.12985

Storto, A., Alvera-Azcárate, A., Balmaseda, M. A., Barth, A., Chevallier, M., Counillon, F., et al. (2019). Ocean reanalyses: Recent advances and unsolved challenges. *Frontiers in Marine Science*, *6*. https://doi.org/10.3389/fmars.2019.00418

Storto, A., Masina, S., & Navarra, A. (2015). Evaluation of the CMCC eddy-permitting global ocean physical reanalysis system (C-GLORS, 1982–2012) and its assimilation components. *Quarterly Journal of the Royal Meteorological Society*, *142*(695), 738–758. https://doi.org/10.1002/qj.2673

Talley, L. D. (2008). Freshwater transport estimates and the global overturning circulation: Shallow, deep and throughflow components. *Progress in Oceanography*, *78*(4), 257–303. https://doi.org/10.1016/j.pocean.2008.05.001

Talley, L. D., Feely, R. A., Sloyan, B. M., Wanninkhof, R., Baringer, M. O., Bullister, J. L., et al. (2016). Changes in ocean heat, carbon content, and ventilation: A review of the first decade of GO-SHIP global repeat hydrography. *Annual Review of Marine Science*, *8*(1), 185–215. https://doi.org/10.1146/annurev-marine-052915-100829

Trenberth, K. E., Jones, P. D., Ambenje, P., Bojariu, R., Easterling, D., Klein Tank, A., et al. (2007). Observations. Surface and atmospheric climate change.

Vinogradova, N. T., & Ponte, R. M. (2017). In search of fingerprints of the recent intensification of the ocean water cycle. *Journal of Climate*, *30*(14), 5513–5528. https://doi.org/10.1175/jcli-d-16-0626.1

Weijer, W., Cheng, W., Drijfhout, S. S., Fedorov, A. V., Hu, A., Jackson, L. C., et al. (2019). Stability of the Atlantic meridional overturning circulation: A review and synthesis. *Journal of Geophysical Research: Oceans*, *124*(8), 5336–5375. https://doi.org/10.1029/2019jc015083

Wett, S., Rhein, M., Kieke, D., Mertens, C., & Moritz, M. (2023a). Meridional Connectivity of a 25-Year Observational AMOC Record at 47°N. *Geophysical Research Letters*, *50*(16), e2023GL103284 https://doi.org/10.1029/2023gl103284

Wett, S., Rhein, M., Kieke, D., Mertens, C., Moritz, M., & Nowitzki, H. (2023b). Basin-wide AMOC volume transport from the NOAC array at 47° N in the subpolar North Atlantic (1993-2018) [Dataset]. *PANGAEA*. https://doi.org/10.1594/PANGAEA.959558

Wijffels, S. E. (2001). Ocean transport of fresh water. In *International geophysics* (Vol. 77, pp. 475–488). Elsevier.

Wijffels, S. E., Schmitt, R. W., Bryden, H. L., & Stigebrandt, A. (1992). Transport of freshwater by the oceans. *Journal of Physical Oceanography*, *22*(2), 155–162. https://doi.org/10.1175/1520-0485(1992)022<0155:tofbto>2.0.co;2

Woodgate, R. A. (2018). Increases in the Pacific inflow to the Arctic from 1990 to 2015, and insights into seasonal trends and driving mechanisms from year-round Bering Strait mooring data. *Progress in Oceanography*, *160*, 124–154. https://doi.org/10.1016/j.pocean.2017.12.007

Wunsch, C. (1996). *The ocean circulation inverse problem*. Cambridge University Press.

Yu, L., & Weller, R. A. (2007). Objectively analyzed air–sea heat fluxes for the global ice-free oceans (1981–2005). *Bulletin of the American Meteorological Society*, *88*(4), 527–540. https://doi.org/10.1175/bams-88-4-527

Zhang, J., & Zhang, R. (2015). On the evolution of Atlantic meridional overturning circulation fingerprint and implications for decadal predictability in the North Atlantic. *Geophysical Research Letters*, *42*(13), 5419–5426. https://doi.org/10.1002/2015gl064596

Zhang, R. (2010). Latitudinal dependence of Atlantic Meridional Overturning Circulation (AMOC) variations. *Geophysical Research Letters*, *37*(16). https://doi.org/10.1029/2010gl044474

Zheng, H. (2024). An observation-based estimate of the Atlantic meridional freshwater transport [Dataset]. *Zenodo*. https://doi.org/10.5281/zenodo.12790901

Zhu, C., & Liu, Z. (2020). Weakening Atlantic overturning circulation causes South Atlantic salinity pile-up. *Nature Climate Change*, *10*(11), 998–1003. https://doi.org/10.1038/s41558-020-0897-7

Zhu, C., Liu, Z., Zhang, S., & Wu, L. (2023). Likely accelerated weakening of Atlantic overturning circulation emerges in optimal salinity fingerprint. *Nature Communications*, *14*(1), 1245. https://doi.org/10.1038/s41467-023-36288-4

Zuo, H., Balmaseda, M. A., Tietsche, S., Mogensen, K., & Mayer, M. (2019). The ECMWF operational ensemble reanalysis–analysis system for ocean and sea ice: A description of the system and assessment. *Ocean Science*, *15*(3), 779–808. https://doi.org/10.5194/os-15-779-2019